Cool Gas in Southern Galaxies

C. HENKEL, Max-Planck-Institut für Radioastronomie, Bonn, Germany
Y.-N. CHIN, Radioastronomisches Institut der Universität Bonn, Germany
R. WIELEBINSKI, Max-Planck-Institut für Radioastronomie, Bonn, Germany
R. MAUERSBERGER, Steward Observatory, Tucson, USA

During the last ten years, the 'Swedish-ESO Submillimetre Telescope' has filled an important astronomical gap. The SEST is by far the largest mm- and submm-wave telescope covering the southern hemisphere and the clear skies of La Silla almost guarantee good weather conditions at 2.6 mm $\lesssim \lambda \lesssim 3.8$ mm. Since 1995, improvements in receiver sensitivity (Schottky receivers were replaced by SIS frontends) and flexibility (two heterodyne receivers can now be used simultaneously) have dramatically altered observing conditions. Complementing its larger cousins of the northern hemisphere (most notably the 30-m IRAM and the 45-m Nobeyama telescopes), the SEST is the only (sub)mm telescope that allows detailed investigations of prominent molecular 'goldmines' like the Magellanic Clouds or CenA. We thus focus on the LMC and the SMC and on two prototypical southern starburst galaxies, NGC 253 and NGC 4945.

The Magellanic Clouds provide an extremely interesting environment to study astrophysical processes. With respect to the molecular interstellar medium, there are three outstanding properties which motivate ongoing research: (1) Metallicities are smaller than in the Milky Way, (2) UV radiation fields are stronger than in the solar neighbourhood, and (3) a large number of targets is found at a well-known (relatively small) distance. The first two properties have far-reaching consequences for the astrophysical and astrochemical state of the interstellar medium: dust depletion and lack of extinction in cloud envelopes result in reduced shielding against UV radiation and decrease the sizes of molecular clouds relative to the more extended neutral atomic gas. Most of the 'intercloud' gas is not molecular but atomic, with HI, not H_2 as the main constituent (e.g. Lequeux et al. 1994). Another aspect of low metallicity is the depletion of molecular abundances relative to H_2 by one order of magnitude (in the LMC) up to two orders of magnitude (in the SMC) (Chin et al., 1998). Since not all elements are depleted by the same amount ([C/H] = –1.3, [O/H] = –0.6 in HII regions and young stars of the SMC) and because the molecular gas is exposed to high UV fields, relative line intensities in the LMC and SMC differ notably from those observed in galactic clouds:

• HCO^+ J=1-0 emission is stronger than HCN J=1-0 emission, reflecting the high ionisation flux that favours HCO^+ while HCN mainly arises from spatially confined and presumably cool cloud cores.

• Relative to ^{13}CO $J = 1$-0, the line emission in the $C^{18}O$ $J = 1$-0 transition is unusually weak. This may be caused by isotope selective photoionisation or by fractionation in a medium with high C^+ abundance. An underabundance of ^{18}O is a third possibility.

• Towards the prominent SMC star-forming region LIRS 36, CN has remained undetected even though a rare CS isotopomer, $C^{34}S$, is seen. In warm galactic clouds, the main CS species tends to emit weaker lines than CN. The non-detection of CN in LIRS 36 is explained in terms of high cloud densities (n (H_2) $\gtrsim 10^5$ cm^{-3}; much of the lower density gas must be atomic) and a (relatively) high fractional abundance of O_2 that is destroying CN but not CS.

To illustrate some of the the observational results, Figure 1 displays CO $J = $ 1-0 and 2-1 emission from the star-forming region N 113 in the LMC. Figure 2 shows HCO^+, HCN, CS, and H_2CO maps. Beamwidths are $25'' \lesssim \theta_b \lesssim 55''$.

Isotope ratios (e.g. Chin et al., 1996; Heikkilä et al., 1998) are also related to abundances, but address stellar nucleosynthesis and 'chemical' evolution. In the LMC, extragalactic deuterium was detected for the first time with certainty. DCO^+ was observed towards the star-forming regions N113, N159, and N44BC, DCN towards N113 and N159 (see Fig. 3 for most of the spectra). HCO^+/DCO^+ and HCN/DCN abundance ratios are 20–70. The data can be used to estimate either the D/H ratio or the electron density of the gas. Because deuterium fractionation depends on small differences in zero-point energies, the process is sensitive to the kinetic temperature. Modeling deuterium chemistry with conditions appropriate for clouds in the LMC, we obtain for T_{kin} ~ 20K a D/H ratio of 1.5×10^{-5} which agrees with the galactic value. The temperatures of the LMC clouds are, however, not that well constrained. The clouds could be slightly warmer (Le-
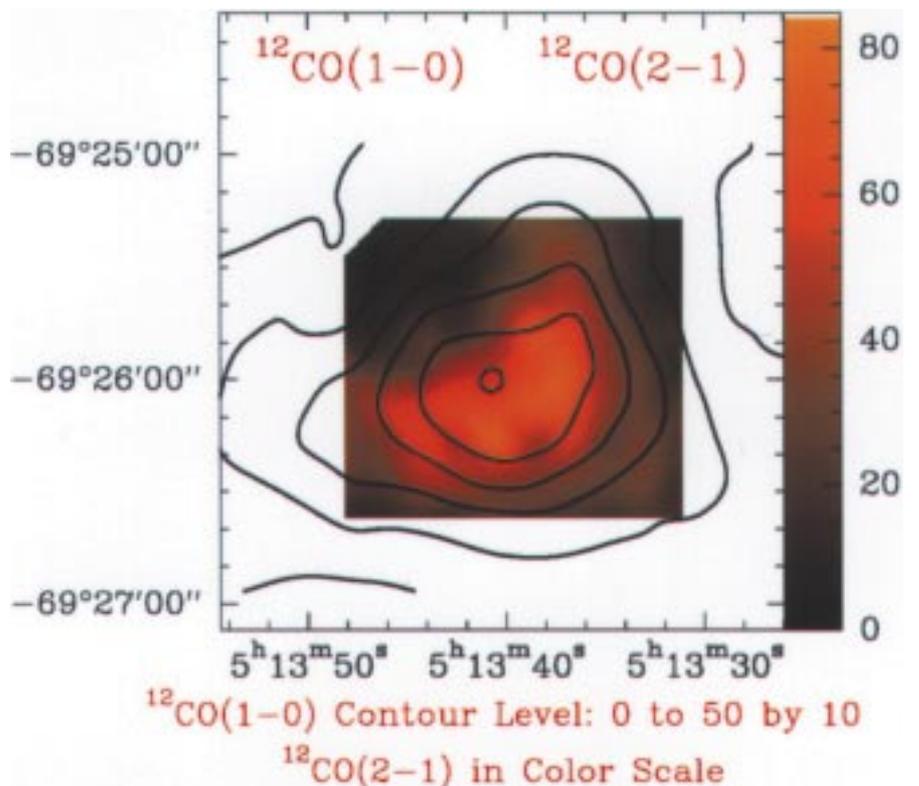
Figure 1: SEST maps of ^{12}CO J=1-0 (contours) and 2-1 line (inserted image) emission from the star-forming region N 113 in the LMC. Angular resolutions are 45″ and 25″, respectively.
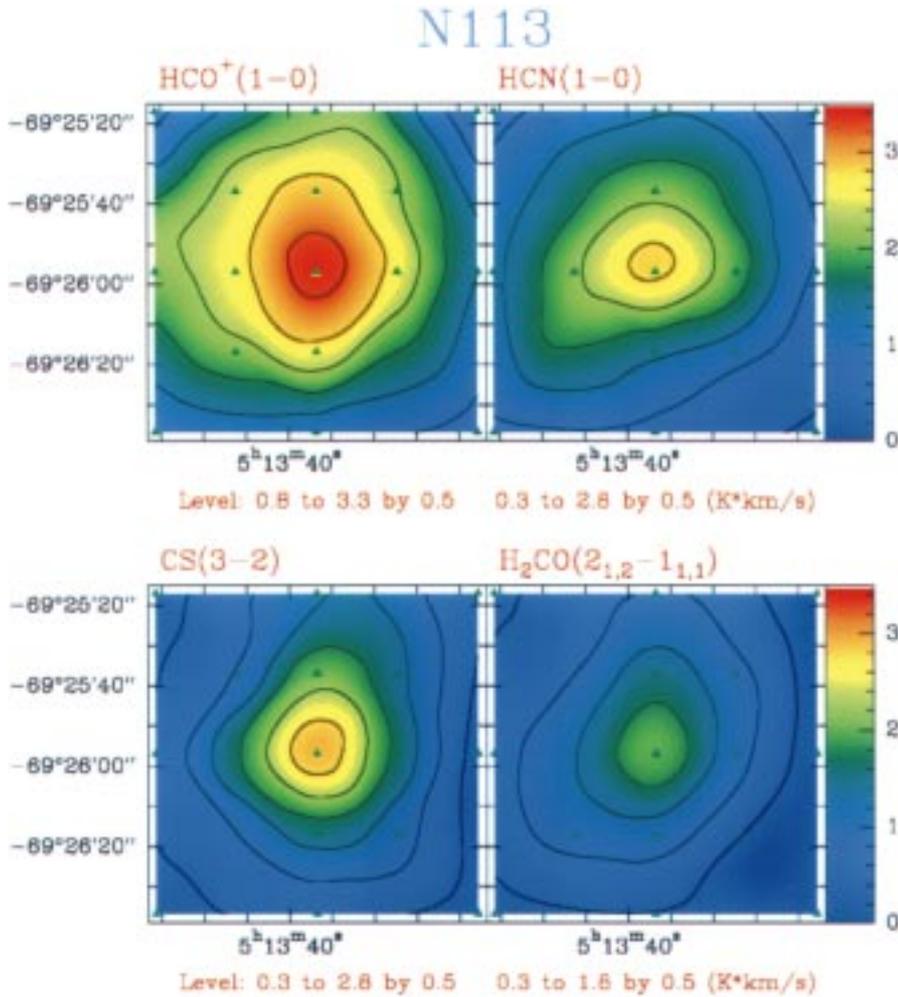
N113

Figure 2: HCO+, HCN, CS, and H2CO emission from N113. Angular resolutions are 55″ for HCO+ and HCN and 35″ for CS and H2CO.

queux et al., 1994) which leads to higher D/H ratios. At a cloud temperature of 30 K, we would need a D/H ratio of about 10 times the galactic value. This would be consistent with the LMC gas being less processed through stars than that of the Galaxy. Irrespective of these considerations, evidence from the LMC is consistent with an open universe as long as the cosmological constant is small.

First attempts to measure CNO isotope ratios were also successful. The interstellar ^{12}C/^{13}C isotope ratio of $\sim$ 50 is similar to that in the inner galactic disk. The ^{18}O/^{17}O isotope ratio, however, differs drastically from the galactic value. It is a factor of two below that measured in the galactic plane and a factor of three below that of the solar system. An interpretation in terms of ^{18}O depletion is possible, but as long as the ^{16}O/^{18}O ratio is not well known, we prefer not to draw conclusions.

Located at a distance of $\sim$ 2.5 Mpc and showing an IRAS PSC flux of $S_{100\mu m}$ $\sim$ 1000 Jy, the edge-on barred spiral **NGC 253** is the brightest member of the Sculptor group showing evidence for starburst activity from radio to X-ray wavelengths. Recent measurements with the SEST (CO J=1-0), the IRAM 30-m telescope (CO J= 2-1), BIMA (CS J= 2-1), and the VLA (H$_2$CO1$_{10}$ − 1$_{11}$) have revealed an extremely complex integrated structural picture of the nuclear region. A progressive change in position angle appears when going from larger to smaller scale sizes approaching the nuclear region. Apparently, the inner region is warped, reflecting perturbations of the
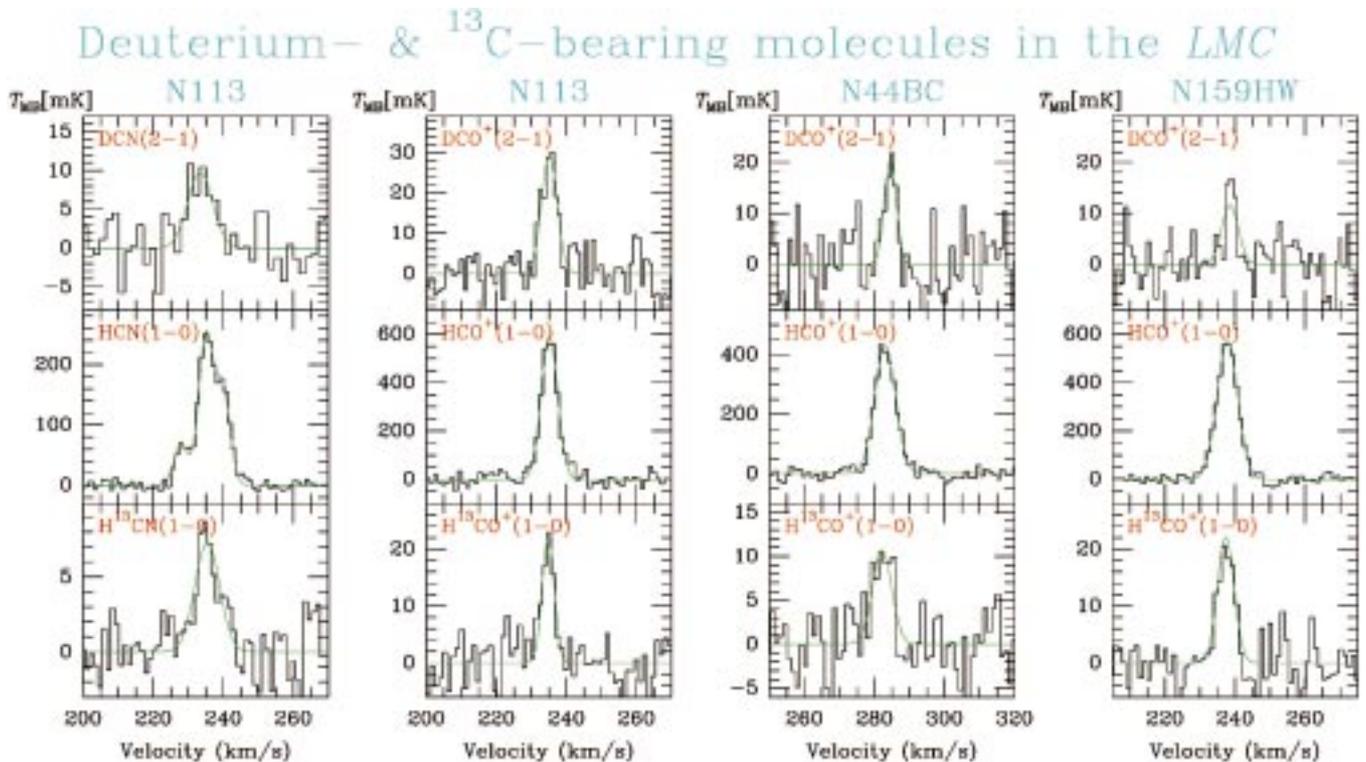
Figure 3: Spectral lines of HCO+ or HCN and their ^{13}C and deuterium bearing isotopomers towards prominent star-forming regions of the LMC. Beamwidths are 35″ for the deuterated and 55″ for the other species.
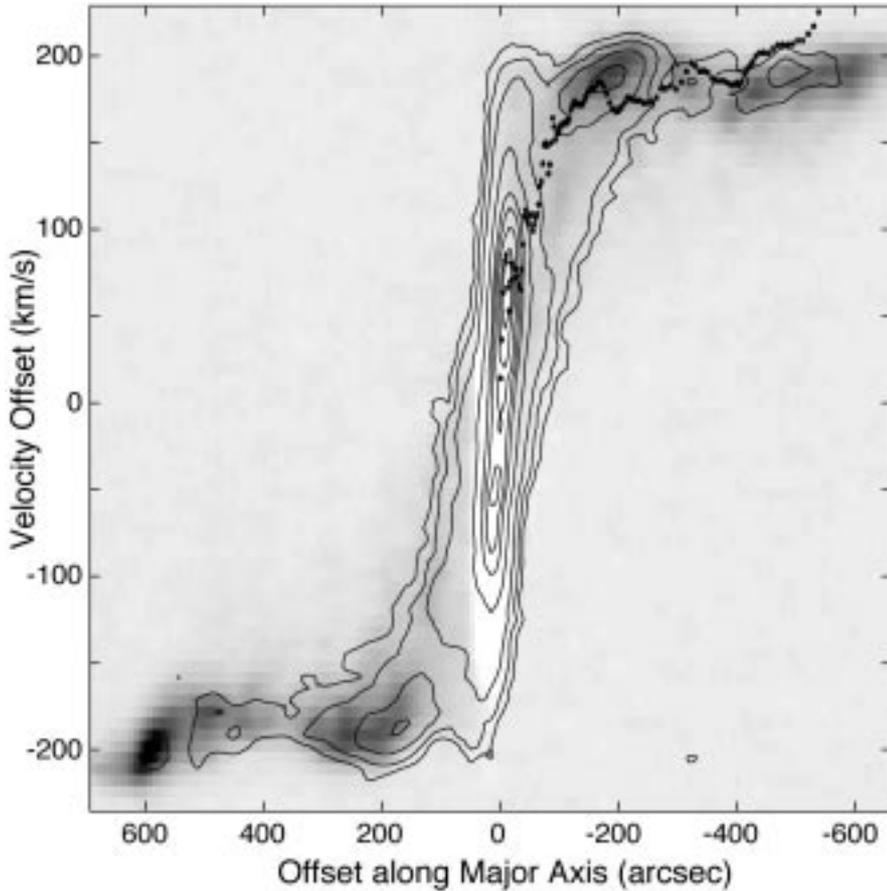
Figure 4: CO J=1-0 (contours), HI (grey scale), and optical (dots) rotation curve of NGC 253. Axes show offsets from $\alpha_{2000} = 00° 47^m 33^s.4$, $\upsilon_{LSR} = 235\ km\,s^{-1}$ (from Houghton et al., 1997).

nuclear region. The following dynamic features can be identified (e.g. Mauersberger et al., 1996b; Baan et al., 1997; Houghton et al., 1997):

• Relatively weak CO emission is associated with the optically visible outer disk at P.A. $\sim 50°$ and is observed out to 11′ (8 kpc) from the nucleus. In the very outer regions the emission is displaced from the major axis and is associated with HI spiral arm features. The intensity ridge shows 'flat' rotation (see Fig. 4).

• An inner CO disk, ridge, bar or spiral with position angle P.A. $\sim 64°$ (Fig. 5) bends back into the outer disk at 120″ (1.5 kpc) on each side of the nucleus. The feature is also seen in the near-infrared and radio continuum.

• The inner 35″ (400 pc) of the galaxy are associated with a rapidly rotating cloud complex enveloping the nucleus. The rotation curve is consistent with solid body rotation (Fig. 4); the velocity gradient is of the order of 0.4 kms^{-1} pc^{-1}, the dynamical mass is 3×10^9 M$_\odot$.

• Even further inside, seen against the triple radio continuum source in the inner 10″, a 'compact' molecular disk with a particularly high velocity gradient (~ 1 km s^{-1} pc^{-1}) is measured at P.A. ~ 36–$39°$ (Fig. 5). This innermost disk structure is observed in OH and H$_2$CO absorption against the nuclear source; it is not seen in molecular emission lines but there is a chain of weak compact

continuum sources with similar position angle. The water vapour emission in NGC 253 might be associated with this compact structure.

• Nuclear outflows with a recessional velocity component above the plane of the optical disk are observed in the OH emission plumes, the radio and far-infra-

red continuum, and possibly in the H$_2$CO data. The plume jets have a P.A. of $\sim -15°$ that is roughly perpendicular to the P.A. $\sim 64°$ ridge (Fig. 5) observed out to $\sim 120″$ from the nucleus.

Comparing ^{12}CO and C^{18}O with 1.3 mm continuum emission, it becomes apparent that the commonly assumed correlation between integrated ^{12}CO intensity and molecular column density, derived from clouds of the galactic disk near the solar circle, does not hold. For the nuclear clouds of NGC 253, molecular masses have to be reduced by almost a factor of ten. This is accompanied by a similar reduction of the gas mass in the central region of the Milky Way. For the inner 410 pc $\times$ 130 pc of NGC 253, $M_{molecular} \sim 5 \times 10^7$ M$_\odot$. We conclude that the nuclear gas mass of NGC 253 is not exceptionally large (a few times that contained in a similar volume in the central region of the Milky Way) and that molecular gas masses in more distant ultraluminous IRAS galaxies may be overestimated. It is the infrared luminosity, not the nuclear gas mass, that makes NGC 253 to be an outstanding galaxy.

NGC 4945 is a nearby edge-on (post-) starburst galaxy with intense infrared, radio, and X-ray radiation from the nuclear region. More than a dozen of molecular species have been detected in this source, most of them with the SEST (Henkel et al., 1994). In addition to a luminous H$_2$O megamaser, the presence of a spatially unresolved molecular ring, seen almost edge-on, has been established by an analysis of ^{12}CO/^{13}CO $J = 1$-0 intensity ratios (Bergman et al., 1992). The ring is characterised by densities of $\sim 10^3$ cm^{-3}; ^{12}CO opacities are of the order of 1–5. The central 80″ $\times$ 80″ of NGC 4945 have been mapped with the SEST not only in
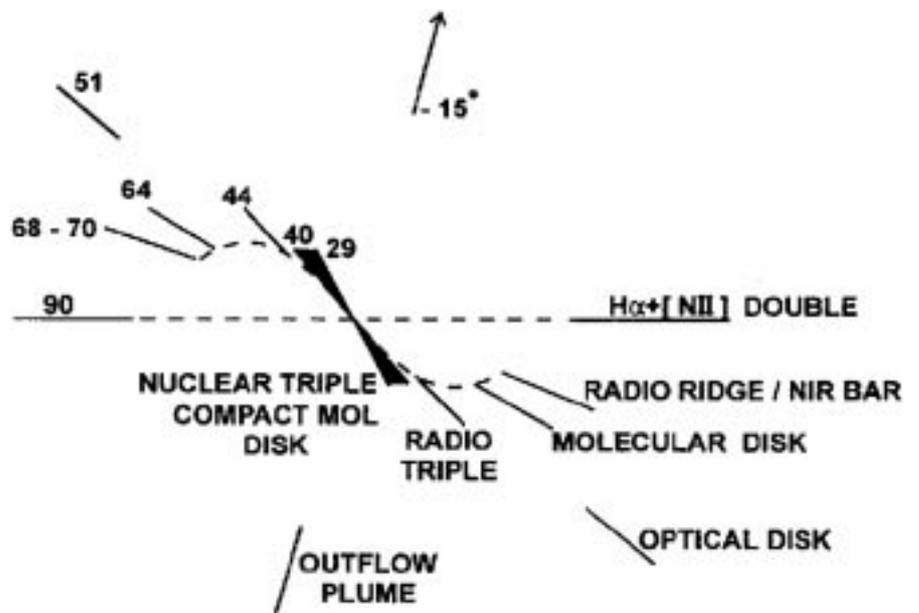
Figure 5: Position angles of major dynamical components of NGC 253 (from Baan et al., 1997).

47

CO J = 1-0 and 2-1 but also in the CO J = 3-2 transition at 870 μm (Mauersberger et al., 1996a). CO J = 3-2 emission is concentrated towards the kinematical centre with a deconvolved full width to half power size of (11.5±3)″, corresponding to a linear scale of (200±50) pc. This is less than the size of the molecular complex seen in the CO J = 1-0 and 2-1 lines. Position velocity maps reveal three condensations located at the centre and at offsets of ± 5″ along the major axis. As in the central regions of the Milky Way and NGC 253, the standard CO intensity – molecular column density conversion factor appears to be too large and the nuclear gas mass becomes ~ 10^8 M$_\odot$. An embedded active nucleus may contribute to the very high 'star-forming efficiency' of L_{FIR}/M_{gas} ~ 150 L$_\odot$/M$_\odot$.

All (sub)millimetre data presented here were obtained with characteristic beamwidths of 15″ – 55″. It is not difficult to imagine that the use of a large multi-element interferometer with ~ 1″ angular resolution would be an enormous qualitative improvement, providing new unprecedented astrochemical tools and leading to detailed views of optically obscured active galactic nuclei.

References

Baan W.A., Bragg A.E., Henkel C., Wilson T.L., 1997, *ApJ* **491**, 134.

Bergman P., Aalto, S., Black J.H., Rydbeck G., 1992, *A&A* **265**, 403.

Chin Y.-N., Henkel C., Millar T.M., Whiteoak J.B., Marx-Zimmer M., 1998, *A&A* **330**, 301.

Chin Y.-N., Henkel C., Millar T.M., Whiteoak J.B., Mauersberger R., 1996, *A&A* **309**, 705.

Heikkilä A., Johansson L.E.B., Olofsson H., 1998, *A&A*, in press.

Henkel C., Whiteoak J.B., Mauersberger R., 1994, *A&A* **284**, 17.

Houghton S., Whiteoak J.B., Koribalski B., Booth R., Wiklind T., Wielebinski R., 1997, *A&A* **325**, 923.

Lequeux J., Le Bourlot J., Pineau de Forêts G., Roueff E., Boulanger F., Rubio M., 1994, *A&A* **292**, 371.

Mauersberger R., Henkel C., Whiteoak J.B., Chin Y.-N., Tieftrunk A.R., 1996a, *A&A* **309**, 705.

Mauersberger R., Henkel C., Wielebinski R., Wiklind T., Reuter H.-P., 1996b, *A&A* **305**, 421.

C. Henkel
p220hen@mpifr-bonn.mpg.de

La Silla, February 1996. In the fading light of the setting sun, two astronomers are watching the moonrise over the high Andes from the SEST. (Photograph: H.-H. Heyer.)